Electronic Versatility of Vanadium in Tris-chelates with Redox-Active Ligands†

*Stephen Sproules**

Spectroscopic and computational examination of the neutral tris-dioxolene complex [V(dbcat)$_3$] (dbcat^{2-} = 3,6-di-*tert*-butylcatecholate) reveals a Class III mixed-valent ground state. The radical is stabilised by delocalisation across the ligands mediated by the energy matched d orbital manifold of the V(V) centre. This electronic structure is compared to the tris-dithiolene and tris-diimine analogues that possess V(IV) and V(II) ions, respectively.

The coordination chemistry of vanadium with redox-active ligands is rather complicated and the actual oxidation levels of the metal and ligands in such species is often quite controversial. Vanadium has an inherent redox flexibility that enables it to accommodate the electronic demands of its ligands. This is most evident in the homoleptic complexes with the archetypal redox-active chelates of dioxolene (derived from catechol), dithiolene and diimine (e.g. bipyridine),[1–3] where the multi-membered electron transfer series is traversed by a concoction of metal and ligand redox steps. This is in stark contrast to the unyielding +III oxidation state of neighbouring chromium that ensures all chemistry is ligand-based.[4,5] The observation produces the well-known *periodic diagonal* of vanadium, molybdenum and rhenium, unified by the similarity of their molecular and electronic structures with these quintessential redox-active chelates.[6]

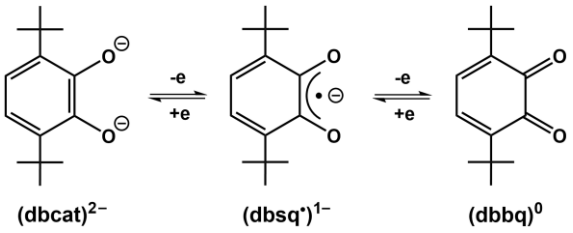

Scheme 1 Oxidation levels of the 3,6-di-*tert*-butylcatecholate ligand

Vanadium tris-dioxolene species extend to a four-membered electron transfer series with the trianionic, dianionic and monoanionic complexes possessing +III, +IV and +V ions, respectively, for the

$[V(Cl_4cat)_3]^z$ (Cl_4cat^{2-} = tetrachlorocatecholate) and $[V(3,5\text{-dbcat})_3]^z$ ($3,5\text{-dbcat}^{2-}$ = 3,5-di-*tert*-butylcatecholate) series.[7,8] The diagnosis was derived from the crystal structure with O–C and C–C bond distances commensurate with the dianionic form of the ligand (Scheme 1). In the absence of a crystal structure for the neutral complex, the assignment remained ambiguous and presented either V(III) with three monoanionic semiquinone radicals or V(V) with one radical and two catecholates. Both scenarios produce a ligand-centred spin which was confirmed by the EPR spectra recorded on $[V(Cl_4cat)_3]$ and $[V(3,5\text{-dbcat})_3]$ with *g*-values of 2.0028 and 2.004, respectively.[7,8] The compounds gave identical ^{51}V ($I = {}^7/_2$, ~100% natural abundance) hyperfine coupling constants, and were subsequently defined as tris-semiquinone species where two ligand spins are strongly antiferromagnetically coupled to the V(III) d^2 ion, such that the EPR spectrum is representative of a *localised spin* on the third ligand.[9] The assignment as a V(III) ion was based on the similarity of the IR spectrum to the neutral Cr analogue, though it was suggested to exist as a V(V) entity in solution produced via internal electron transfer for which catecholate complexes are renowned.[10]

The assessment was improved recently with the crystallographic characterisation of $[V(dbcat)_3]$ ($dbcat^{2-}$ = 3,6-di-*tert*-butylcatecholate) where the repositioning of ^{t}Bu substituents stabilised the complex toward aerial oxidation that limited the $[V(3,5\text{-dbcat})_3]$ analogue.[11] The bond metrics were consistent with one $dbsq^{1-\bullet}$ and two $dbcat^{2-}$ ligands coordinating a V(V) ion (Scheme 1). The complex was assigned as possessing Class I ligand mixed valency based on the crystallographic two-fold axis,[12] an arrangement said to persist in solution with the EPR spectrum yielding hyperfine coupling constants of 4.53 G to the two ligand protons and 3.47 G to ^{51}V nucleus.[11] The number of hyperfine lines and the magnitude of the coupling constants generates a simulated spectrum considerably wider than the experimental data. Moreover it is unclear how the V(V) d^0 ion could induce localisation of a radical in the absence of an exchange interaction. A re-evaluation was undertaken considering a delocalised spin which yielded a ^{51}V

coupling of -2.18×10^{-4} cm^{-1}, which is a better match with literature values (Fig. S1). In addition coupling to six ligand protons at 2.92×10^{-4} cm^{-1}, a value consistent with 3.2 G coupling for protons in the free benzosemiquinone.[13] Careful modelling of the lineshape gave a near perfect simulation of the fluid solution spectrum reinforcing the assignment as [V^{V}(dbcat)$_2$(dbsq$^{\bullet}$)] with Class III ligand mixed valency,[12] in line with the assessment for tris-dioxolene species from theoretical calculations.[9,14]

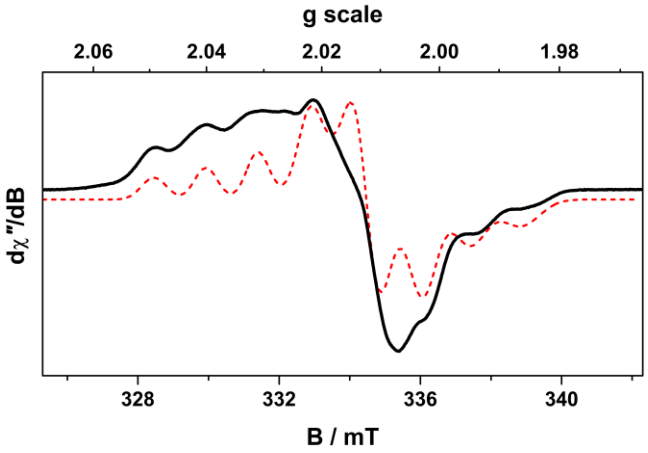

Fig. 1 X-band EPR spectrum of [V(dbcat)$_3$] recorded in toluene solution at 30 K. The simulation is shown in red with the experimental spectrum in black (experimental conditions: frequency, 9.4206 GHz; power, 0.63 mW; modulation, 0.2 mT).

The frozen solution spectrum presented in Fig. 1 is dominated by the ^{51}V hyperfine interaction. The extremes of the signal are readily identified as belonging to one component of the *A*-matrix. The simulation gave g = (2.014, 2.017, 2.009) and A = (2.0, –13.9, 2.0) $\times 10^{-4}$ cm^{-1}. The two small, positive components of the hyperfine were estimated from the average obtained from the isotropic spectrum and represent a best fit to the signal. Spectral resolution is compromised by aggregation of the analyte, most noticeably in the middle of the signal leading to a mismatch in intensities compared with the ends of the spectrum. The issue was not remedied by dilution, nor mixing solvents or adding an electrolyte (e.g.

tetraalkylammonium salt) to separate out the molecules. The same issue befell an isoelectronic tris-aminophenolate complex which also gave a featureless signal at 60 K.[15] Overall the spectrum is very similar to related complexes with benzoseminquinone ligands bound to Co(III),[16] which are similarly interpreted with an isotropic *g* and axial *A*, where only one component is clearly visible. Moreover the hyperfine coupling of ^{59}Co is about the same as that here for ^{51}V, which reaffirms the assignment as a radical ligand coordinated to a diamagnetic metal ion given both isotopes have the same spin, natural abundance and Larmor frequency. Any contribution to the signal from coupling of the ligand protons is obscured by line broadening.

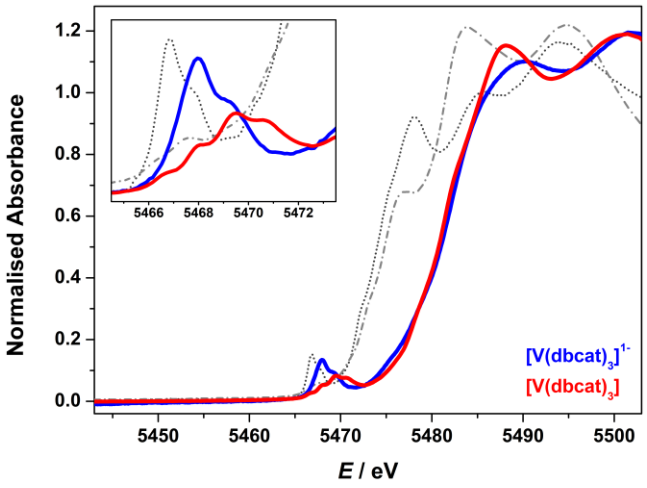

Fig. 2 Comparison of the normalised V K-edge X-ray absorption spectra of [V(dbcat)$_3$] and Na[V(dbcat)$_3$]. The inset shows expansion of the pre-edge region. The spectra for [V(edt)$_3$] (dotted line) and [V(^{t}bpy)$_3$] (dash-dot line) are provided for reference.

The V K-edge X-ray absorption spectra for [V(dbcat)$_3$] and Na[V(dbcat)$_3$] are overlaid in Fig. 2. The salient observation is the rising edge energy attributed to dipole-allowed 1s → *n*p transitions that offer a direct measure of the effective nuclear charge at vanadium.[3] These edges are almost superimposed, with

the inflection point at 5480.8 eV for [V(dbcat)$_3$] and 5481.0 eV for Na[V(dbcat)$_3$], unambiguously showing both V ions have the same oxidation state. This assessment can only be made when the compounds have very similar coordination spheres, e.g. VO_6. This point is made by inclusion of the V K-edge spectra of [V(edt)$_3$] and [V(^{t}bpy)$_3$] in the plot showing their rising-edge 6.6 eV lower in energy at 5474.2 eV.[2,3] These compounds are isoelectronic with [V(dbcat)$_3$] but have distinctly different electronic structures, with a V(IV) ion in the tris-dithiolene and a V(II) ion in the tris-diimine, formulated as [V^{IV}(edt$_3^{4-}$)] and [V^{II}(^{t}bpy$^{\bullet}$)$_2$(^{t}bpy)], respectively. Both are vanadium-centred paramagnets as defined by EPR spectra in stark contrast with the tris-dioxolene analogue (Table S1). Given a change of ~1 eV in the edge energy is considered an indication for a change of oxidation state by one unit, there is a dramatic shift in edge energies with a change in donor atoms. The larger sulfur donors in [V(edt)$_3$] have a better energetic match to the 3d manifold resulting in a trigonal prismatic geometry that maximises π-overlap with the the metal. As a result, the softer ligands make the vanadium centre easier to ionise than complexes with hard dioxolene ligands. The nitrogen donors in 2,2′-bipyridine are also described as hard ligands, however they will be reduced especially when paired with early transition metals unwilling to support a large number of d-electrons,[17] like the formal V(0) d^5 centre in [V(^{t}bpy)$_3$]. The exact position of the edge in [V(^{t}bpy)$_3$] is difficult to define because of the additional structure in the rising-edge from unresolved transitions to higher p states of the metal and low-lying π* states inherent to bipyridine ligands.

Pre-edge features *ca*. 10 eV below the rising edge stem from dipole forbidden but quadrupole-allowed 1s → 3d transitions. In addition to providing a measure of oxidation state, their number and intensity is defined by coordination number and geometry (Fig. 2 inset). Two pre-edge peaks separated by 1 eV are clearly resolved for Na[V(dbcat)$_3$], with the more intense feature at lower energy (Table 1). On the other hand, [V(dbcat)$_3$] as four pre-edge peaks. The middle two peaks match the energy of those for Na[V(dbcat)$_3$]. The first peak resides at 5466.9 eV and has the weakest intensity but is positioned beneath

the onset of the first pre-edge peak for Na[V(dbcat)$_3$]. The fourth peak is the highest in energy at 5470.5 eV. The first three peaks are designated as transitions to 3d orbitals in a trigonal ligand field ($a_1 < e < e$). The final pre-edge peak could result from photodamage to the sample during the measurement as the neutral complex is more susceptible than the highly robust monoanionic species.[7,8]

Table 1 Experimental and calculated V K-pre-edge transition energies

		transition energies[b]	
	transition[a]	**experimental**	**calculated[c]**
[V(dbcat)$_3$]	1s → a_1 (d_{z^2})	5466.9	5466.8
	1s → 3e (d_{xy,x^2-y^2})	5468.2	5468.0
	1s → 4e ($d_{xz,yz}$)	5469.5	5469.5
[V(dbcat)$_3$]$^{1-}$	1s → a_1 (d_{z^2})		5467.0
	1s → 3e (d_{xy,x^2-y^2})	5468.0	5468.1
	1s → 4e ($d_{xz,yz}$)	5469.0	5469.9

[a] Largest contribution to calculated pre-edge peak. [b] In eV. [c] Shifted by +38.87 eV.

The geometry optimised structure of [V(dbcat)$_3$] in the gas phase produced several changes compared with the crystal structure.[11] Most noticeable is the homogeneity of the intraligand bond lengths giving three identical ligands (Table S11). The average C–O and aromatic C–C distances of 1.325 Å and 1.411Å, respectively, are the result of Class III behaviour for formally one benzosemiquinone and two catecholate ligands which is typical in complexes with ligand mixed valency.[1,5] The optimisation has flattened the ligands which are folded along the O···O vector by almost 15° in the crystal structure, and the overall geometry is slightly more trigonal prismatic as defined by a twist angle, $\Theta = 41°$. This suggests lattice forces between adjacent molecules and solvation, in addition to the two-fold crystallographic axis conspire to produce a charge localised depiction of the complex in the solid state. The optimised structure

of the monoanion resulted in a slight lengthening of the average C–O bond to 1.339 Å commensurate with three dianionic catecholate ligands about a V(V) central ion. Although the solid state structure of Na[V(3,5-dbcat)$_3$] has been reported, it exists as dimer where the Na^+ counterions are part of second coordination sphere,[7,18] precluding any comparison.

Tris-dioxolene complexes possess a three-fold axis, splitting the d orbitals split into one nondegenerate a_1 – the nonbonding d_{z^2} orbital – and two sets of degenerate e orbitals (d_{xy,x^2-y^2} and $d_{xz,yz}$), that participate in π- and σ-bonding, respectively, with the ligands. The ground state electronic structures for [V(dbcat)$_3$] ($S = {}^1/_2$) and $[V(dbcat)_3]^{1-}$ ($S = 0$) were calculated using the B3LYP hybrid functional and showed the lowest unoccupied orbital (LUMO) as the nonbonding a_1 (d_{z^2}) orbital such that both complexes possess a V(V) d^0 ion (Figs S2 and S3). The highest occupied orbitals (HOMO) are the three ligand π orbitals that transform as a_2 and e in C_{3v} symmetry. The Mulliken spin density plot sees +1.91 spins distributed over the three ligands with a –0.91 on vanadium (Fig. S13). The spin density at the metal stems from polarisation of the six V–O bonds brought about by coordination of hard donor atoms to a highly Lewis acidic metal ion, and is well-documented.[3,19] Although the distribution is more asymmetric for the crystallographic structure of [V(dbcat)$_3$], the unpaired electron is still delocalised over the three ligands (Fig. S13). In $[V(dbcat)_3]^{1-}$ with three catecholate ligands, these orbitals are filled. Oxidation to neutral [V(dbcat)$_3$] results the a_2 orbital being singly-occupied (SOMO) and the provenance of the Class III mixed valency. Broken symmetry calculations were applied to these complexes in order to analyse the potential energy surface that could give rise to alternative ground state configurations (Table S12). For [V(dbcat)$_3$], the BS(3,2) calculation, which represents a V(III) ion coordinated by three benzosemiquinone radicals, converged to the V(V) solution (Fig. S6). This is due to the miniscule $d_{xy}/d_{x^2-y^2}$ contribution to the corresponding ligand e_π orbitals, which is in stark contrast to the composition of these orbitals in $[V^{II}(^t bpy^{\bullet})_2(^t bpy)]$.[2] The BS(1,1) calculation on $[V(dbcat)_3]^{1-}$ gave a solution comprising a very weak

overlap of the metal a_1 and ligand a_2 magnetic orbitals (Fig. S8). This result is formulated $[V^{IV}(dbcat)_2(dbsq^{\bullet})]^{1-}$, and resides 7.9 kcal mol^{-1} above the spin-restricted state, though this reduces to 4.6 kcal mol^{-1} when electron withdrawing substituents are added to the ligand periphery, i.e. $[V(Cl_4cat)_3]$ (Table S12).

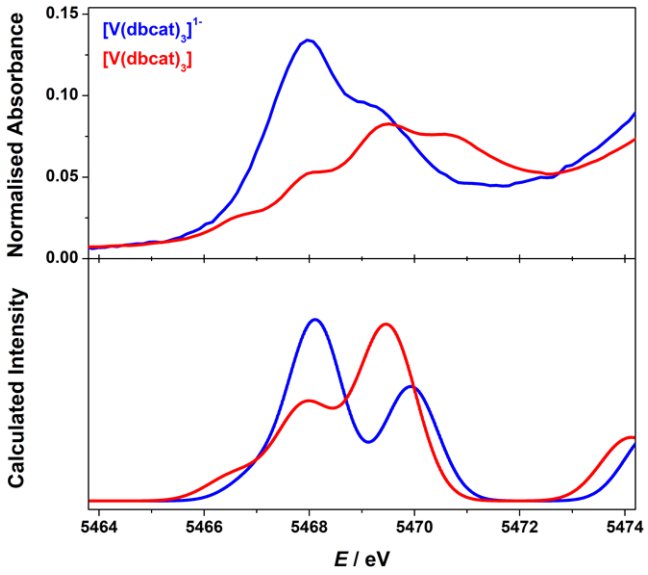

Fig. 3 Experimental (top) and calculated (bottom) V K-pre-edge spectra for $[V(dmcat)_3]$ and $[V(dmcat)_3]^{1-}$ obtained from B3LYP TD-DFT calculations. Calculated intensity in arbitrary units.

The theoretical models are verified by the accurate reproduction of the pre-edge features using time-dependent (TD)-DFT calculations (Fig. 3).[2,3] The first three peaks of $[V(dbcat)_3]$ are calculated within 0.2 eV of the experimental values (Table 1). These are assigned as sequential transitions into unoccupied d_{z^2}, d_{xy,x^2-y^2} and $d_{xz,yz}$ orbitals (Fig. S20), where the intensity is proportional to vacancies in the acceptor levels and the dipole contribution provided by p-d mixing (Table S13). There is no transition probability for an excitation to the a_2 SOMO as it has no vanadium character, and the fourth peak plausibly arises from photodamage or decomposition as all available transitions for $[V(dbcat)_3]$ are assigned. Three transitions

are also calculated for $[V(dbcat)_3]^{1-}$ though the first peak is obscured by the more intense transition to the d_{xy,x^2-y^2} orbitals, which have more 4p character (Fig. S21). Interestingly the splitting between these two peaks is the same as for $[V(dbcat)_3]$. The third pre-edge peak is the excitation $d_{xz,yz}$ orbitals, and the calculated energy is overestimated by 0.9 eV, but the relative intensity is an excellent match with the experiment.

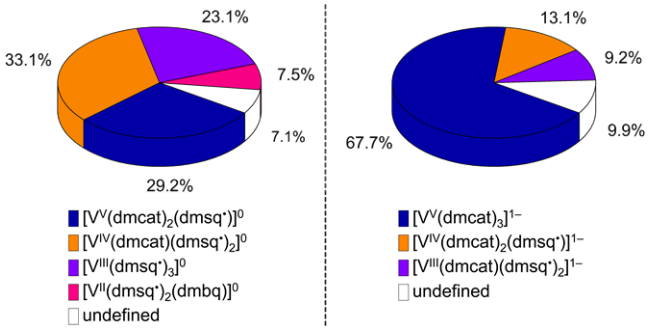

Fig. 4 Configurational ground state compositions from analysis of CAS wavefunctions for $[V(dmcat)_3]$ and $[V(dmcat)_3]^{1-}$.

Given the debate over the electronic structure of neutral tris-dioxolene complexes as either V(V) with one benzosemiquinone or V(III) with three ligand radicals,[7–9,15,20] the ground state compositions of the neutral and monoanionic species was investigated using correlated post-Hartree-Fock *ab initio* calculations. A reference space of ten orbitals encompassing the 3d manifold and their ligand-centred counterparts was chosen. For this exercise, the ^{t}Bu substituents were downsized to methyl groups, giving $[V(dmcat)_3]$ and $[V(dmcat)_3]^{1-}$ (Figs S15 and S16). The ground state of the monoanion is two-thirds V(V) with three catechol ligands, matching the most stable configuration from DFT (Fig. 4). There are contributions from V(IV) and V(III) configurations also consistent with broken symmetry calculations. The neutral complex has a ground state comprising an equal mix of V(V), V(IV) and V(III) configurations. This is concordant with DFT where the BS(3,2) converges to the UKS solution, and primarily stems from an increase in V

3d contribution to the π-bonding orbitals. Both the DFT and CASSCF results give <10% d_{xy,x^2-y^2} content to these orbitals, and largely independent of the ligand substituents. The results are verified by analysing the ground state composition of isoelectronic tris-dithiolene and tris-diimine species, where the former is 74% [$V^{IV}(edt_3^{4-})$] and the latter 66% [$V^{II}(^t bpy^{\bullet})_2(^t bpy)$], neatly reflecting the experimental data.[2,3]

With the electronic structure experimentally and computationally defined as [$V^{V}(dbcat)_2(dbsq^{\bullet})$] via direct measurement of the oxidation state, there is need to clarify the missing intervalence charge transfer (IVCT) band that is diagnostic of ligand mixed-valency.[1,5] Both [$V(dbcat)_3$] and [$V(dbcat)_3]^{1-}$ are blue compounds because of the dominant absorption band at 670 nm and 625 nm, respectively.[11,18] This is a defined as a ligand-to-metal charge transfer (LMCT) excitation from the ligand e_π to the predominantly metal e_{π^*} orbitals. Tris-dithiolene analogues also have an intense absorption in the range 650 – 750 nm which is assigned as an IVCT excitation into the ligand-centred a_2 orbital.[3] Here the geometry influences the energy of this transition, and the intensity a consequence of the larger 3p orbitals and associated spin-orbit coupling of sulfur. On the other hand, [$V(^t bpy)_3$] has an IVCT band at ~2200 nm, and the expectation is that [$V(dbcat)_3$] would have a similar low-energy band as seen with Cr analogues.[5,14] However the IVCT transition for vanadium will occur at a higher energy because there is considerably less 3d content to the ligand e_π orbitals (<10%), and the intensity is attenuated due to the half-occupancy of the a_2 acceptor orbital. Therefore it would likely appear to lower energy though obscured by the LMCT band.[11] The fact that is not observed underpins the electronic structure assignment and highlights an accurate calculation of the orbital composition where the 3d manifold of the V(V) ion is more energetically separated from the ligand π orbitals. For early transition metals that aspire to their highest oxidation state, fully reduced dioxolenes are required as a ligand field that maximises π donation is preferrable to any additional stability gained from coordinated dioxolene radicals.

This work is based in part on research conducted at the Stanford Synchrotron Radiation Lightsource (SSRL), which is supported by the U.S. DOE, Office of Science, Office of Basic Energy Sciences, under Contract DE-AC02-76SF00515. The Structural Molecular Biology Program is supported by the U.S. DOE, Office of Biological and Environmental Research, and by NIH/NIGMS (P30GM133894).

Notes and references

WestCHEM, School of Chemistry, University of Glasgow, Glasgow G12 8QQ, UK. E-mail: stephen.sproules@glasgow.ac.uk

†Electronic supplementary information (ESI) available: Experimental and computational methodology, spectra, and computational data. See DOI: 10.1039/c000000x/

References

1 C. G. Pierpont, *Inorg. Chem.*, 2011, **50**, 9766.

2 A. C. Bowman, S. Sproules and K. Wieghardt, *Inorg. Chem.*, 2012, **51**, 3707.

3 S. Sproules, T. Weyhermüller, S. DeBeer and K. Wieghardt, *Inorg. Chem.*, 2010, **49**, 5241.

4 C. G. Pierpont, *Inorg. Chem.*, 2001, **40**, 5727.

5 R. R. Kapre, E. Bothe, T. Weyhermüller, S. DeBeer George, N. Muresan and K. Wieghardt, *Inorg. Chem.*, 2007, **46**, 7827.

6 S. Sproules and K. Wieghardt, *Coord. Chem. Rev.*, 2011, **255**, 837.

7 M. E. Cass, N. R. Gordon and C. G. Pierpont, *Inorg. Chem.*, 1986, **25**, 3962.

8 M. E. Cass, D. L. Green, R. M. Buchanan and C. G. Pierpont, *J. Am. Chem. Soc.*, 1983, **105**, 2680.

9 D. J. Gordon and R. F. Fenske, *Inorg. Chem.*, 1982, **21**, 2907.

10 (*a*) C. G. Pierpont, *Coord. Chem. Rev.*, 2001, **216-217**, 99; (*b*) C. G. Pierpont, *Coord. Chem. Rev.*, 2001, **219-221**, 415.

11 A. M. Morris, C. G. Pierpont and R. G. Finke, *Inorg. Chem.*, 2009, **48**, 3496.

12 M. B. Robin and P. Day, *Adv. Inorg. Chem. Radiochem.*, 1967, **10**, 247.

13 O. Ryba, J. Pilař and J. Petránek, *Collect. Czech. Chem. Commun.*, 1968, **33**, 26.

14 G. H. Spikes, S. Sproules, E. Bill, T. Weyhermüller and K. Wieghardt, *Inorg. Chem.*, 2008, **48**, 10935.

15 H. Chun, C. N. Verani, P. Chaudhuri, E. Bothe, E. Bill, T. Weyhermüller and K. Wieghardt, *Inorg. Chem.*, 2001, **40**, 4157.

16 (*a*) S. L. Kessel, R. M. Emberson, P. G. Debrunner and D. N. Hendrickson, *Inorg. Chem.*, 1980, **19**, 1170; (*b*) C. W. Lange, B. J. Conklin and C. G. Pierpont, *Inorg. Chem.*, 1994, **33**, 1276.

17 (*a*) A. C. Bowman, J. England, S. Sproules, T. Weyhermüller and K. Wieghardt, *Inorg. Chem.*, 2013, **52**, 2242; (*b*) J. England, C. C. Scarborough, T. Weyhermüller, S. Sproules and K. Wieghardt, *Eur. J. Inorg. Chem.*, 2012, 4605; (*c*) C. C. Scarborough, S. Sproules, T. Weyhermüller, S. DeBeer and K. Wieghardt, *Inorg. Chem.*, 2011, **50**, 12446.

18 C.-X. Yin and R. G. Finke, *J. Am. Chem. Soc.*, 2005, **127**, 9003.

19 M. Nicolaou, M. G. Papanikolaou, A. C. Tsipis, T. A. Kabanos, A. D. Keramidas, S. Sproules and H. N. Miras, *Chem. Eur. J.*, 2018, **24**, 3836.

20 S. R. Cooper, Y. B. Koh and K. N. Raymond, *J. Am. Chem. Soc.*, 1982, **104**, 5092.